Rain–Snow Boundaries over Southern Ontario

RONALD E. STEWART AND PATRICK KING

Atmospheric Environment Service, Downsview, Ontario, Canada M3H 5T4

(Manuscript received 10 February 1986, in final form 9 February 1987)

ABSTRACT

Rain–snow boundaries in two southern Ontario storms are examined. Radar and satellite information were used to illustrate the nature and extent of the associated precipitation and cloud regions. The deepest radar echoes and clouds occurred close to the boundary. Surface temperature and pressure were related to the boundary; some of the changes in these parameters were shown to be attributable to melting snowflakes. These radar, satellite, and surface observations are consistent with a mesoscale circulation driven by melting snow.

1. Introduction

Canadian winter storms commonly produce both rain and snow. The boundary between these two forms of precipitation, the rain–snow boundary, is consequently an inherent storm characteristic. Transportation can be severely disrupted in the adjacent snow region, whereas water runoff can be a hazard in the adjacent rain region.

The rain–snow boundary also presents a difficult forecasting problem. Traditionally, forecasts have relied upon predicted critical thickness values in the lower troposphere. Lamb (1955) used the 1000–500 mb thickness value, whereas, for example, Koolwine (1975) used the 1000–850 mb thickness. In practice, these techniques provide only a general guide to the location of the boundary. An improved understanding of the phenomenon can lead to a better numerical simulation of it as well as better real-time identification techniques.

The atmospheric conditions in the vicinity of the boundary must be such that snow entirely melts on one side of the boundary, partial melting occurs in the boundary region to produce a mixture of rain and snow, and no melting occurs on the other side. Understanding the melting process of snow is therefore critical to understanding the rain–snow boundary. Lumb (1961) and others showed that a few hundred meters are required for snow to melt in temperatures up to 2°–3°C. Lamb (1955) further pointed out that larger flakes require greater distances to melt. The size of the snow is however a function of the environment through which it falls. Large 0°C layers in the rain–snow boundary region (Koolwine, 1975) will allow significant aggregation to occur and thus lead to larger flakes (Stewart et al., 1984; Stewart, 1984). Several studies by Japanese investigators (e.g., Matsuo and Sasyo, 1981a,b,c) developed equations to quantify the melting rates of snowflakes. As well, Matsuo et al. (1981) described atmospheric conditions associated with snow and rain in Japanese storms.

The diabatic process of melting also affects the temperature of the atmosphere. Findeisen (1940) first showed that the process of melting commonly produces 0°C layers in the atmosphere. Subsequently, several authors (Wexler et al., 1954; Wexler, 1954; Atlas et al., 1969; Stewart et al., 1984) have shown that this cooling can be significant. Stewart (1984) showed that some 0°C layers can exceed 1 km in depth. As pointed out by Wexler et al. (1954), cooling of the air by melting can also cause snow to fall in regions where initially only rain fell.

This coupling between microphysical and thermodynamic processes will also affect mesoscale dynamics. Atlas et al. (1969) showed that wind perturbations in raining systems can be driven by melting. Leary and Houze (1978) showed that melting (with evaporation) affected mesoscale downdrafts in tropical systems. Heymsfield (1979) suggested that wind fields in warm frontal bands were affected by melting, whereas Carbone (1982) suggested that melting influences the dynamics of cold frontal circulations. Marwitz (1983) showed that melting influences orographic flows, and Lord et al. (1984) demonstrated that melting is an important link between cloud microphysical processes and mesoscale dynamics. Lin and Stewart (1986) predicted that a mesoscale circulation should also be linked to the rain–snow boundary as well.

Despite the growing awareness of the effects of melting upon related phenomena, the nature of the rain–snow boundary has not been adequately addressed. It appears that only two published papers have even mentioned the physical processes occurring in the boundary. Wexler et al. (1954) presented some information on the boundary in support of their assertion that melting could have affected the near-surface temperature field, and Matsuo et al. (1981) described some

surface precipitation characteristics in raining or snowing regions.

Consequently, the objectives of this article are to describe the mesoscale and surface features that occur in the vicinity of a rain–snow boundary and to show that melting snow affects some of these features. These objectives will be accomplished through the use of satellite, radar, rawinsonde, and surface observations for two case studies.

2. Case study: 13 May 1984

A low-pressure system formed on a trailing cold front in South Dakota at 0000 UTC 13 May 1984. The low moved ESE in response to upper-level steering to eastern Pennsylvania by 0000 UTC 14 May. Throughout this period, the central pressure was nearly constant at about 1010 mb and the circulation around the low remained fairly weak (Fig. 1).

Precipitation began as showers and thunderstorms, but by 1200 UTC 13 May reports indicated mostly light continuous rain and no snow. As the precipitation area moved eastward, snow was reported from several Ontario stations.

The sounding data for Buffalo show the conditions which prevailed during the 12 h period as the precipitation area approached and crossed southern Ontario (Figs. 2 and 3). There was significant cooling above 850 mb, warming in a layer around 900 mb, and cooling near the surface. At 00 UTC (two-digit hours hereafter), the Buffalo hodograph shows warm air advection up to 3 km.

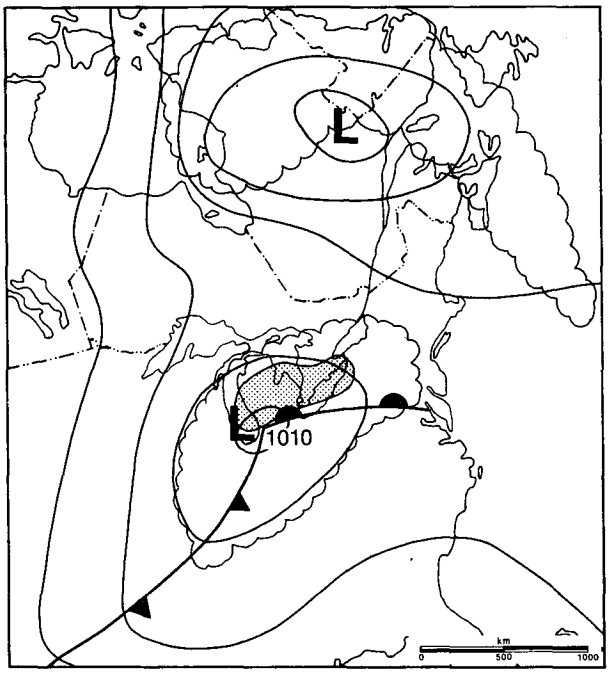

FIG. 1. The surface synoptic chart for 18 UTC 13 May 1984. Isobars are every 4 mb.

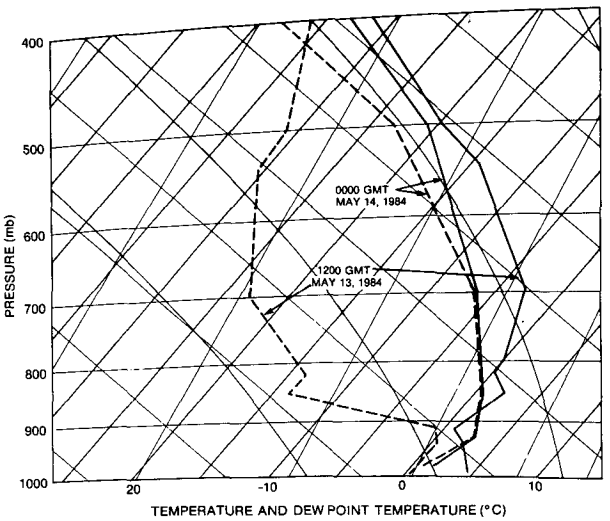

FIG. 2. A tephigram showing the temperature and dewpoint temperature profiles at 12 UTC 13 May 1984 and at 00 UTC 14 May 1984 from Buffalo, New York. The straight and curved lines running from the lower right to the upper left are dry and saturated adiabats, respectively. The heavy and solid lines running from the lower left to the upper right are isotherms and isopleths of saturation mixing ratio (g kg^{-1}), respectively.

Koolwine (1975) found the 1314 m 1000–850 mb thickness line to be associated with the rain–snow boundary over southern Ontario. Snow should occur for thicknesses less than this value and rain for greater thicknesses. At 12 UTC the 1314 m line ran from northern Michigan through London, Ontario to Buffalo. The precipitation area was entirely to the south of the line. Only rain was falling and this is consistent

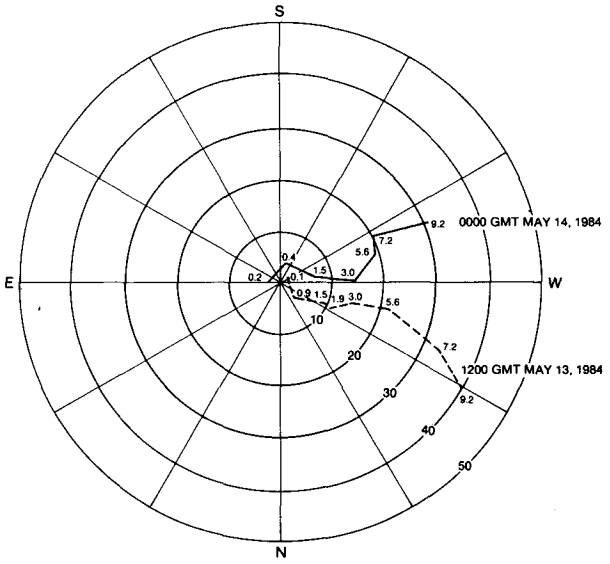

FIG. 3. Wind hodograph for soundings on 13 and 14 May 1984 from Buffalo. Heights are expressed in kilometers and wind speeds are in m s^{-1}.

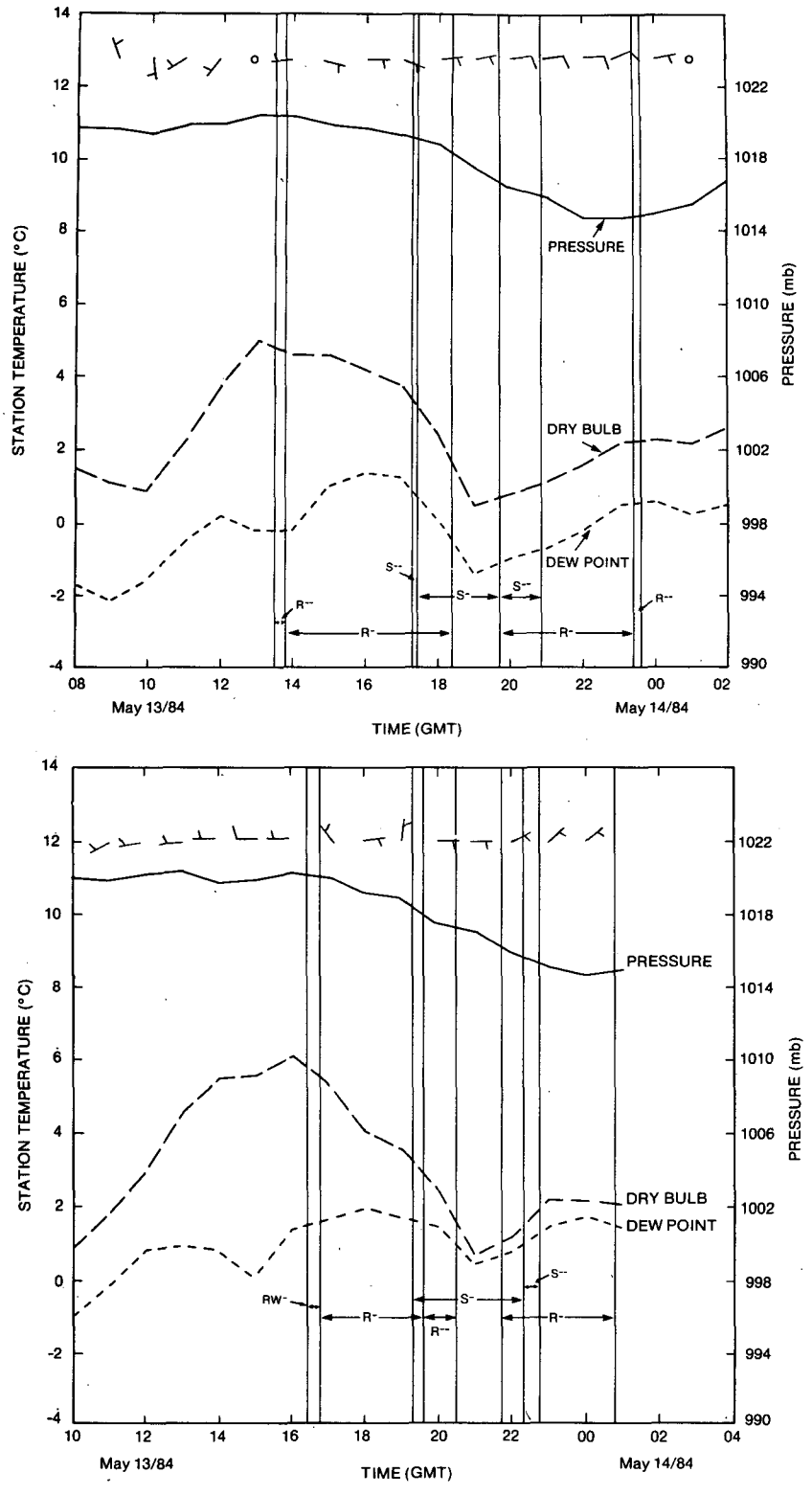

FIG. 4. Surface parameters plotted as a function of time at (a) London, (b) Hamilton, and (c) Toronto on 13 and 14 May 1984. Short and long barbs on the wind vectors indicate 2.5 and 5.0 m s^{-1}, respectively. The symbol L denotes drizzle, R denotes rain, RW denotes rain showers, F denotes fog, and S denotes snow. Two dashes accompanying one of these symbols indicates very light, one dash indicates light, and a plus indicates heavy.

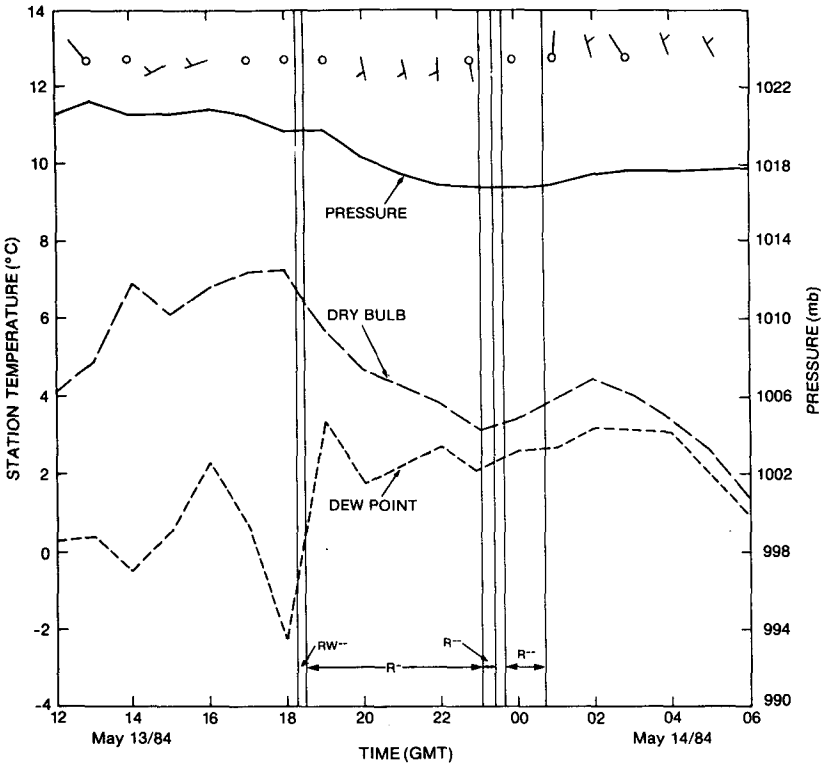

FIG. 4. (*Continued*)

with the prediction. By 00 UTC 14 May, it was slightly south of its 12 UTC location and it ran from Detroit to Rochester and then northward. Some snow was reported north of the line.

This southerly movement occurred in a region of warm air advection. The necessary cooling to counteract this warming may have been caused by diabatic effects or by vertical motion. In section 4, estimates of the relative importance of these contributions will be made.

Soundings from Buffalo are illustrated in Fig. 2. At 12 UTC 13 May, the 0°C level was at 820 mb, although 0°C was almost reached again at 910 mb. This sounding was made in advance of the precipitation and shows considerable subsaturation above 900 mb. By 00 UTC 14 May, after precipitation had occurred, the atmosphere was essentially saturated below 700 mb.

Light precipitation fell over southern Ontario (Fig. 4). There were reports of very large snowflakes at London (its location is shown in Fig. 5). As reported in the Toronto Globe and Mail newspaper, snowflakes were as large as "silver dollars," that is, approximately 3.5 cm in diameter. The predicted occurrence of deep layers having temperatures close to 0°C near the rain–snow boundary would provide an ideal environment for the production of such large aggregates (Stewart et al., 1984; Stewart, 1985).

The temperature traces at the sites varied with precipitation type (Fig. 4). As precipitation commenced, temperatures were approximately 5°C at London, 6°C at Hamilton, and 7°C at Toronto. Surface temperatures then immediately began to decrease at all sites. The largest 1 h declines were associated with the onset of snow at the surface at the two western sites as temperatures there lowered to less than 1°C. In contrast, the surface temperature at Toronto, where rain fell, only decreased to 3°C. Snow fell at both the western sites for over 1 h. As the temperature later rose, a mixture of snow and rain fell. Because the temperature during the snow period fell below the dewpoint at previous times, not all of the drop in temperature can be explained by evaporation.

Pressure changes were linked to precipitation transitions. Pressure decreased over the period of the observations except for slight rises just as precipitation ended. A brief leveling of the pressure occurred with or just before the onset of snow at London and Hamilton. The largest pressure drop at London occurred during the transition from snow to rain.

Two radar displays from the 5 cm wavelength radar at Exeter are shown in Fig. 5. At 1834 UTC, the highest reflectivities, in excess of 42 dBZ_e, were oriented NW–SE, and the leading edge of this high reflectivity region was just west of London. By 2034 UTC, the region with reflectivities in excess of 42 dBZ_e was not as well organized, but it was still generally oriented NW–SE.

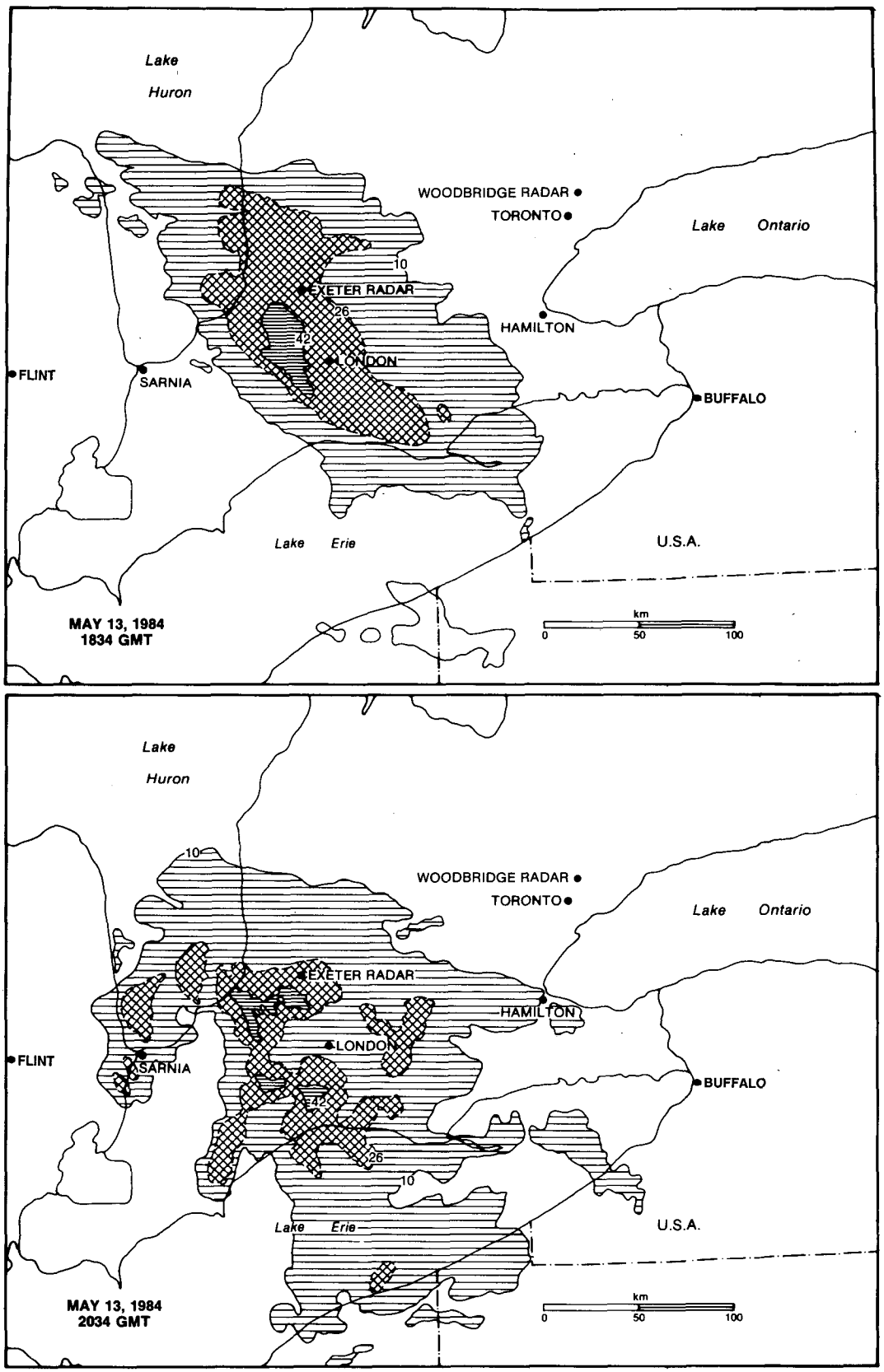

FIG. 5. Two CAPPI radar plots from the Exeter radar on 13 May 1984. Reflectivities are expressed in dBZ_e.

After 2034 UTC, the area of precipitation steadily decreased. At 00 UTC, the weak remaining echoes were aligned WSW–ENE.

The orientation of the highest reflectivity echoes was similar to that of the winds. As shown previously in Fig. 3, winds above approximately 1 km were NW at 12 UTC and backed afterwards until they were SW at 00 UTC on 14 May. The alignment of the radar echoes after 2034 UTC also underwent this same backing.

The motion of the precipitation regions was difficult to determine because of their evolution. An estimated value was 15 m s^{-1} from the SW or W. This value suggests that the precipitation region moved with low level (<3 km) winds rather than with the winds at higher levels.

The vertical radar reflectivity as a function of time over London is illustrated in Fig. 6. Detectable echoes reached 5.5 km near 1825 UTC which approximately corresponded with the onset of a period of snow. The echo top decreased continuously over the entire snow period. The echoes in the only-rain region after 21 UTC were almost distinct features as opposed to the more continuous regions that were present previously. Most of the high reflectivity values occurred at low levels, although at 1845 UTC there was an elevated region of high reflectivities.

The production of large semi-melted snowflakes within the melting layer may explain the high reflectivity observations at low levels. Consequent enhanced reflectivities, called the radar bright band, have been studied by many authors since Ryde (1946). As shown by Battan (1973), reflectivities in rain of 42 dBZ_e correspond to rainfall rates of about 10 mm h^{-1} as opposed to the observed light rainfall rates which would be a maximum of about 2.5 mm h^{-1}. For this explanation to account for the enhanced reflectivity near 1845 UTC, an elevated region having temperatures at or above 0°C must have been present.

Satellite information is also plotted in Fig. 6. In agreement with the radar observations, the infrared data (converted to height) indicate that the highest clouds were associated with the initial transition from rain to snow at 1830 UTC. The estimated cloud top height was 9 km at this time, considerably higher than measured by the radar. This apparent discrepancy in heights is probably just a consequence of the minimum detectable signal of the radar.

The relationship between precipitation type and surface conditions has recently been investigated by Matsuo et al. (1981). These authors used routine surface data from three weather stations in Japan to obtain relationships between the type of precipitation on the ground and other surface meteorological information such as temperature, relative humidity, and rainfall rate. As shown in Fig. 7, they found that temperature and relative humidity were of primary importance in delineating precipitation type. As would be expected, warmer temperatures lead to higher probabilities of rain. Because of the role of evaporative cooling in retarding the onset of melting at a given temperature (e.g., see List and Dussault, 1967), the likelihood of rain increases with relative humidity. Matsuo et al. also

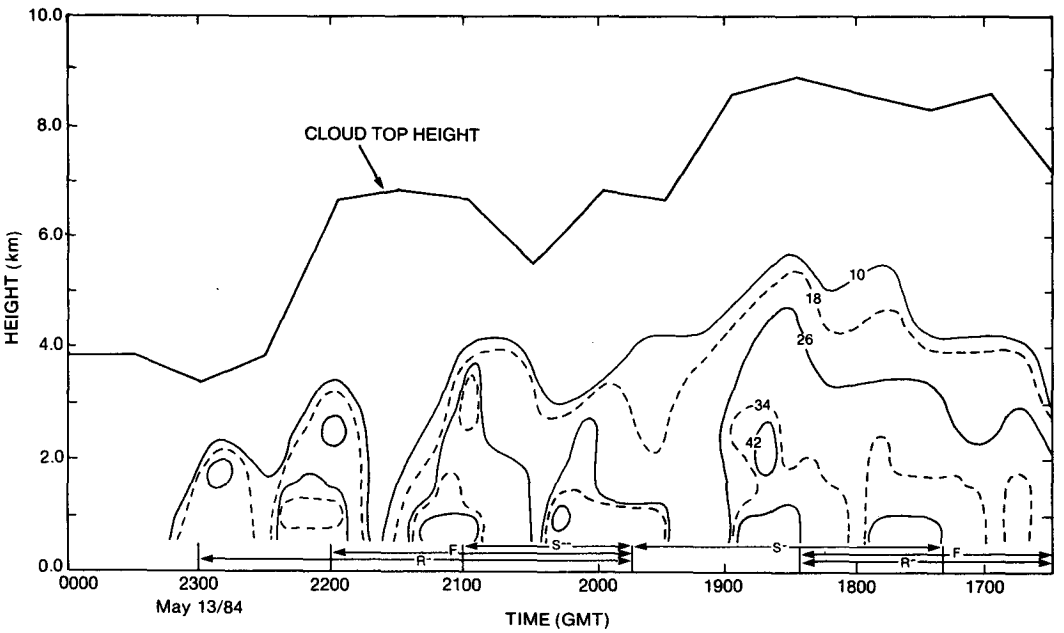

FIG. 6. The vertical radar reflectivity over London as a function of time on 13 May 1984. Infrared information from the GOES-East satellite as well as surface information are also indicated. Using the 00 UTC sounding from Buffalo on 14 May, satellite-derived temperatures have been converted to heights. The coding for the surface parameters is the same as described in Fig. 4.

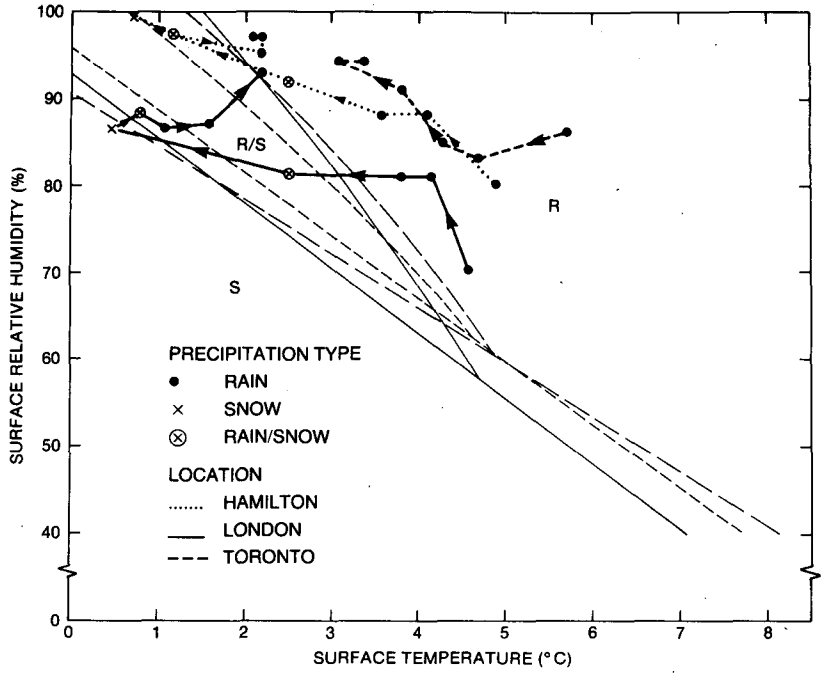

FIG. 7. The relationship between predicted and observed precipitation type and surface temperature and relative humidity. The observed surface precipitation type evolution (Fig. 4) is plotted sequentially for each of the southern Ontario sites. Empirical curves to delineate precipitation type, as determined by Matsuo et al. (1981), are indicated by the three light lines. These light lines refer to results that Matsuo et al. found at three locations in Japan. In this Japanese study, only rain was observed in the R region, only snow was observed in the S region, and a mixture of rain and snow was observed in the R–S region.

showed that the onset of a mixture of rain and snow depends somewhat on precipitation rate. At a higher precipitation rate, larger snowflakes are expected (Gunn and Marshall, 1958). At a given temperature and relative humidity, these will melt more slowly than smaller snowflakes. Consequently, the occurrence of mixed precipitation is directly proportional to precipitation rate.

Because snow spectra tend to be relatively independent of location (Gunn and Marshall, 1958), the Japanese results should also be consistent with the southern Ontario observations. As expected (Fig. 7), the southern Ontario observations generally agreed with the boundaries of the Japanese work, but there were some differences. Rain occurred well within the mixed precipitation region at London, whereas snow fell in the mixed precipitation sector and mixed precipitation fell in the rain region at Hamilton. The Japanese work stated that no such departures occurred in their cases.

3. Case study: 6 December 1983

The synoptic situation in the 6 December case (Fig. 8) was quite different from the 13 May case. The storm developed in the Mississippi Valley on the east side of a major trough. It deepened rapidly as it passed south of the lower Great Lakes. The central pressure fell 32 mb in the 24 h period beginning at 12 UTC 6 December. This storm therefore easily qualifies as a bomb (Sanders and Gyakum, 1980). In contrast to the previous case, there was strong warm air advection ahead of the storm and strong cold air advection in its wake.

Temperature and wind information near the track of the storm is illustrated in Figs. 9 and 10. At 00 UTC on 6 December, the atmosphere was almost saturated below 800 mb, and veering winds, indicating warm air advection, were present in this lower region. At 12 UTC, there was an approximate isothermal layer of 2°C from the surface to 830 mb. Veering winds were still present in this lower layer. The effect of the warm air advection is evident in the warming below 800 mb. By 00 UTC 7 December, the low-pressure center had passed east of Buffalo, and there was considerable drying in the midtroposphere. The midlevel drying east of the surface cold front is consistent with a split cold front (Browning and Monk, 1982).

The surface observations at London and Toronto on 6 December illustrated consistent features (Fig. 11). At both locations, the entire period was characterized by nearly saturated conditions with respect to water. Transitions to and from snow occurred during periods of lowering and rising temperatures, respectively. Although the entire period was characterized by decreasing pressures, a steadying of the pressure occurred dur-

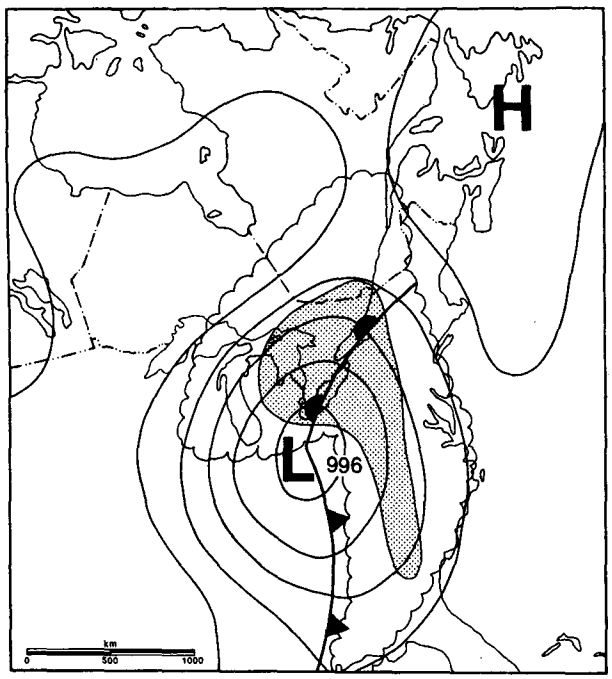

FIG. 8. The surface synoptic analysis for 12 UTC on 6 December 1983. Isobars are every 4 mb.

ing the initial onset of snow. The steepest declines in pressure were closely associated with the transition from snow to rain.

Two radar CAPPI displays from the 5-cm wavelength radar at Woodbridge are shown in Fig. 12. Significant radar echoes persisted from approximately 03 UTC 6 December to 02 UTC 7 December. Over this period the maximum values on the 1.5 km CAPPI displays were approximately 42 dBZ_e, but these values only occurred within small regions on a few of the displays. Banded features in the rain region south of the radar were apparent at 12 UTC. The alignment of the banded features was NE–SW which was, as in the 13–14 May case, roughly parallel to the winds above about 1 km.

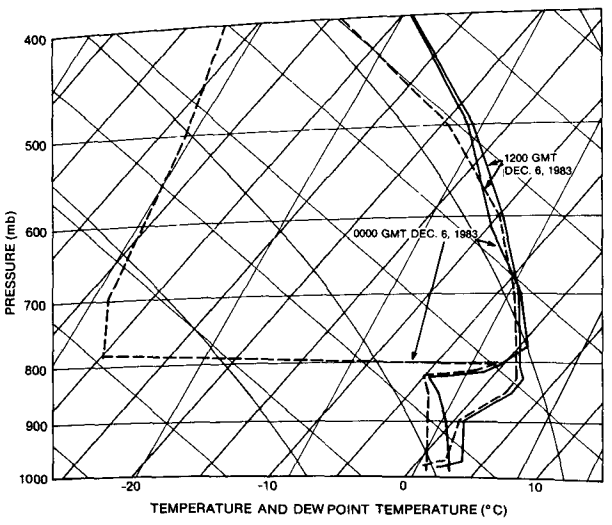

FIG. 9. A tephigram showing the temperature and dewpoint temperature profiles at 00 and 12 UTC 6 December 1983 from Buffalo. The information is plotted in the same manner as in Fig. 2.

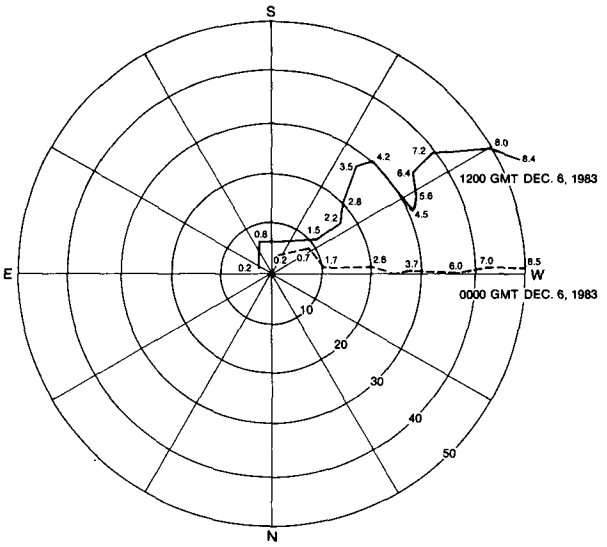

FIG. 10. Wind hodographs for soundings on 6 December 1983 from Buffalo. Heights are expressed in kilometers and wind speeds are in m s^{-1}.

The precipitation region moved slowly. By examining a series of radar plots, it was determined that the precipitation features moved perpendicular to their alignment or NW at approximately 10 m s^{-1}. High reflectivity regions within these features moved along the length of the features; this corresponds to velocities from 240° at approximately 15 m s^{-1}. The hodograph information from Buffalo at 12 UTC indicated that SE winds only occurred in the lowest 1 km. The SW winds at higher levels only had values of 15 m s^{-1} in the 1.5–2.0 km range of heights. Therefore the alignment of the precipitation features was roughly perpendicular to the low-level winds and parallel to the winds above the 1.5 km level. The motion of the embedded features was similar to the winds in the 1.5–2.0 km layer, at least as measured on the 12 UTC sounding.

The vertical radar reflectivity as a function of time over Toronto illustrates additional aspects of the precipitation region (Fig. 13). First, the radar echoes were significantly higher during the rain and rain with snow periods than during the snow only periods. These heights decreased continually in the snow region from the initial rain–snow transition near 05 UTC and they increased after 12 UTC when rain only or snow with rain occurred. Second, the highest reflectivities generally occurred in the rain or rain with snow regions. The heavy snow regions were, however, associated with reflectivities greater than 34 dBZ_e. Third, a distinct

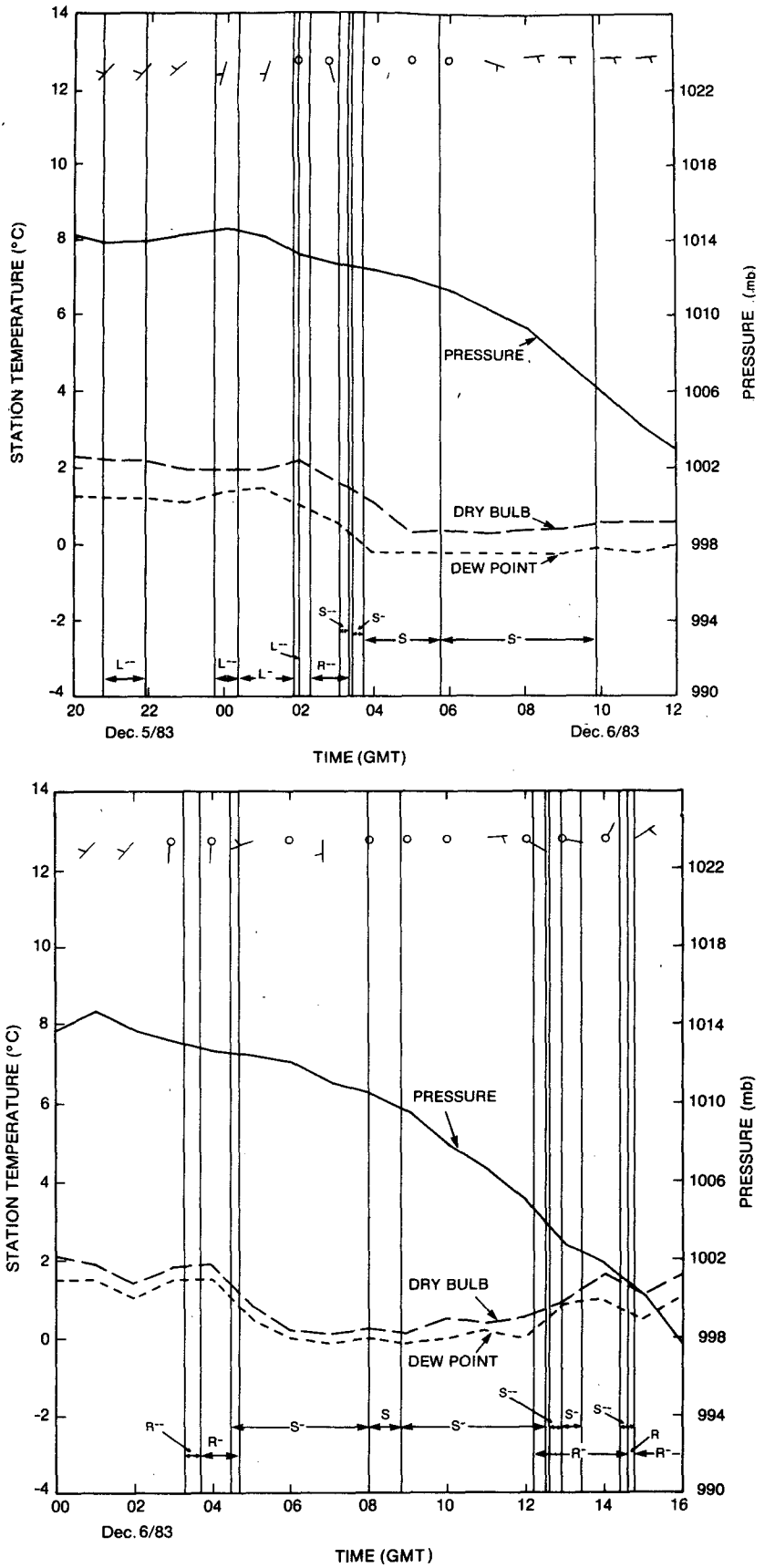

FIG. 11. Surface parameters plotted as a function of time at (a) London and (b) Toronto on 6 December 1983. The coding for these surface parameters is the same as described in Fig. 4.

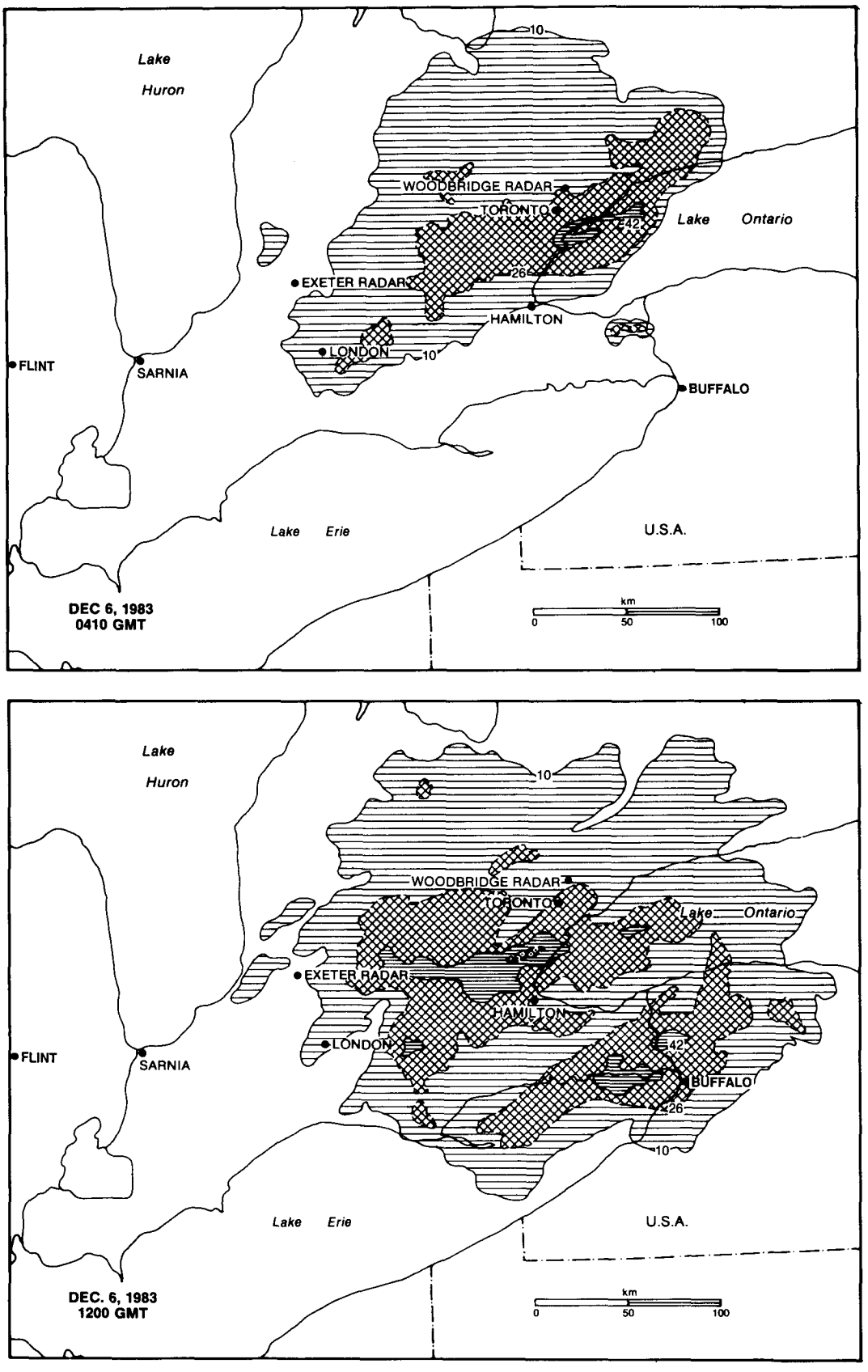

FIG. 12. Two CAPPI radar plots from the Woodbridge radar on 6 December 1983. Reflectivities are expressed in dBZ_e.

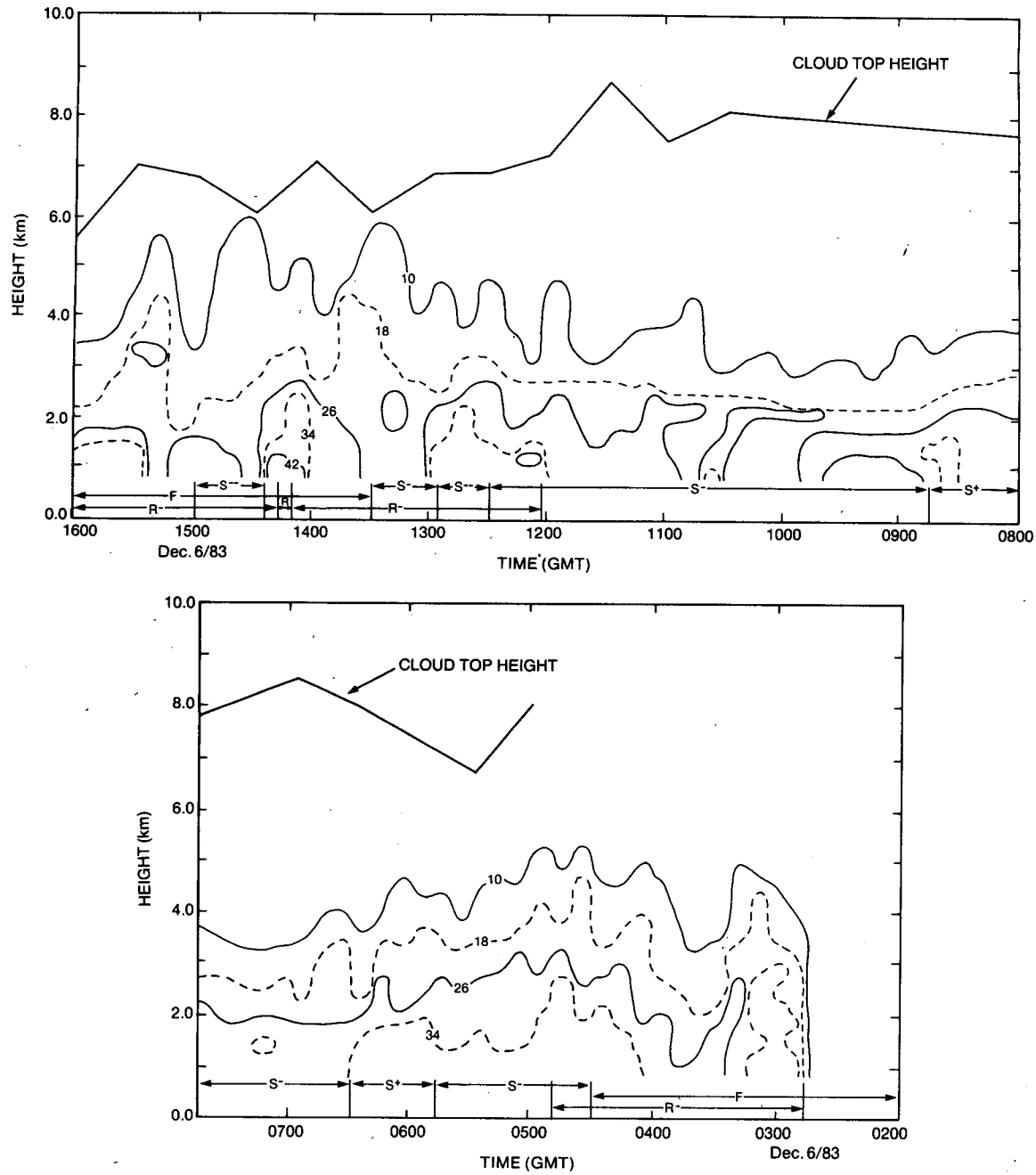

FIG. 13. The vertical radar reflectivity profile over Toronto as a function of time on 6 December 1983. Infrared information from the GOES-East satellite as well as surface precipitation type are also indicated. Using the 12 UTC sounding from Buffalo on 6 December, satellite-derived temperatures have been converted to heights. The coding for the surface parameters is the same as described in Fig. 4.

bright band was not observed in the rain cases, possibly because information was not available from low enough radar scans. However, the change to mixed precipitation from snow at 12 UTC was characterized by the abrupt onset of reflectivities below 2 km that were higher by 4–8 dB than in the adjacent snow-only region. A similar but not as distinct a trend occurred near the 2 km level during the onset of snow near 05 UTC. The wetting of snowflakes prior to their collapse would contribute 6 dB to the measured reflectivities (Battan, 1973).

GOES-East information reveals a relationship between cloud top and transitions of precipitation type at the ground (Fig. 13). The highest clouds occurred

just before the transition from snow to rain at 12 UTC. Deeper radar echoes in subsequent raining regions were, however, associated with generally lower clouds. Unfortunately, satellite data were not available before 05 UTC, and therefore values during the initial rain to snow transition could not be examined.

The relation between temperature and relative humidity during the precipitation episode at Toronto was also examined. The snowfall occurred completely within the predicted mixed phase portion of the Matsuo et al. (1981) diagram, whereas the rain and mixed phase observations were consistent with the predictions.

4. Discussion of observations

The rain–snow boundaries in the two cases illustrate similarities in their mesoscale structure. When rain first evolved into snow at the surface, radar echo tops reached their maximum heights. The maximum height of the radar reflectivities decreased steadily with increasing distance (and time) into the only snow region. This latter point was especially noticeable in the 6 December case. Here, snow was long-lived. Similarities also occurred in association with the transition from snow to rain. The precipitation in the following rain (or mixed precipitation) areas was normally organized into bands and/or convective regions; this was not the case in the snow regions.

Rain–snow boundaries are therefore regions of nonuniform cloud organization. Even at heights of several kilometers there are patterns correlated with surface precipitation type. As evidenced by some of the radar data, such as on 13–14 May, the precipitation regions are also evolving over periods of the order of a few hours.

The width of the rain–snow boundaries varied. In the 13 May case, two boundaries occurred at both London and Hamilton. Using the onset times of the boundaries at the two sites, the component of their velocity along the line joining the sites was approximately 15 m s^{-1}. The first rain–snow boundary required 65 min to pass over London and 71 min to pass over Hamilton. The width was therefore approximately constant at 60 km. In contrast, the second boundary required 43 min to pass over London and 73 min to pass over Hamilton. Its width therefore increased from about 38 to 64 km; its rate of increase was about 4 m s^{-1}. In the 6 December case, only the first boundary at London could be clearly related to a rain–snow boundary passage at Toronto. This boundary approximately maintained its 11 km width between the sites. The weak storm system of 13 May was therefore characterized by constant or widening rain–snow boundaries, whereas the more intense and deepening system of 6 December was characterized by at least one boundary having an approximately constant width and being significantly narrower than the 13 May boundaries.

In general, the changes in temperature near the surface in association with rain–snow boundaries are a consequence of horizontal advection, vertical motions, and diabatic processes. Ideally, the relative contribution of each of these terms should be accurately determined. However, the available rawinsonde information is only sufficient to provide a comparison of the orders of magnitude of the terms. In the 14 May case and using the hodograph and thermal wind equation, the rate of warming due to horizontal advection in the layer below 700 mb was estimated to be 2 K/12 h. Assuming a vertical motion of 30 mb/12 h, the rate of cooling due to vertical motion was estimated to be 1.5 K/12 h. For an assumed 10 mm of precipitation and applying the cooling equation first developed by Atlas et al. (1969), the cooling due to melting snow was estimated to be 3 K/12 h. The advective and vertical motion terms oppose each other, whereas the melting term is at least as large as either of the other terms. These estimates are consistent with the hypothesis that the southward extension of the snow was significantly affected by the melting snow itself. Similar results were also found in the 6 December case. The magnitude of the three terms in this case were 3 K/12 h for warm air advection, 2.5 K/12 h for vertical motion (assuming ascent of 40 mb/12 h) and again 3 K/12 h for 10 mm of precipitation. In both cases, these estimates suggest that melting was a significant factor in the cooling of the lower atmosphere.

A more detailed comparison can be made for the diabatic term. The amount of snow required for a temperature profile to evolve into the deep 0°C layer that should be present at the rain–snow boundary can be estimated. Assume that the initial temperature profile is shown in Fig. 14. Assuming further that the cooling of the air is due only to melting, as previously done in similar cases by Atlas et al. (1969) and Stewart (1984), the conservation of energy leads to:

$$D = c_p\rho_a[(T_1 - T_0)(z_3 - z_2) + 2(T_1 - T_0)(z_2 - z_0) + (T_2 - T_1)(z_2 - z_1) + (T_3 - T_1)(z_1 - z_0)]/2L_f\rho_w \quad (1)$$

where D is the equivalent depth of rain at the surface, c_p is the specific heat capacity of the air, ρ_a is the average air density in the layer, ρ_w is the density of water, and L_f is the latent heat of fusion. The heights z and the temperatures T are indicated in Fig. 14. It should be noted that this formula may overestimate the amount of precipitation required to initiate snow since snow can fall before surface temperatures drop to 0°C.

Atmospheric cooling by melting snow can alone explain a significant portion of the surface temperature observations. In the 13 May case, the Buffalo soundings indicate that equivalent depths of rain of approximately 12 and 9 mm are required for the 0°C layer to form at 12 UTC on 13 May and 00 UTC on 14 May, respectively. Before snow only fell, Hamilton received 7.2 mm of rain and London received 9.6 mm. Similar

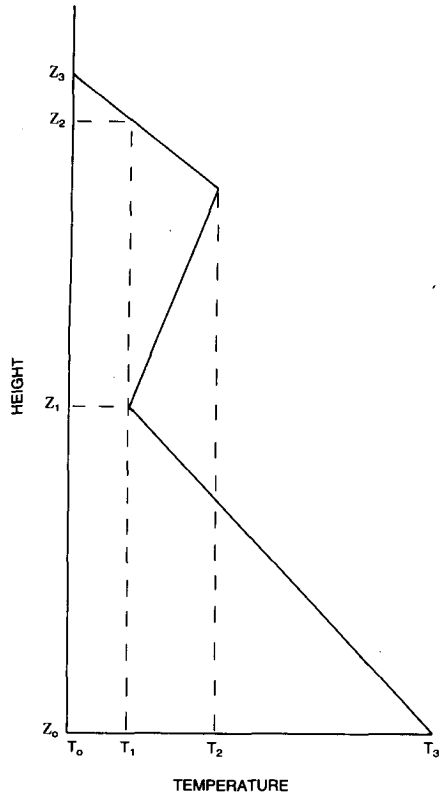

FIG. 14. Schematic diagram indicating the general temperature profile that was used for determining the amount of precipitation required to cool the atmosphere to a deep 0°C isothermal layer.

comparisons for the 6 December case could not be made because precipitation gauges were not operated past 1 December at the stations of interest. From Eq. (1), the needed precipitation amounts ranged from approximately 2 to 12 mm.

The cases also illustrated similarities in surface pressure and wind. Superimposed onto general pressure falls of 0.5–1.0 mb h^{-1}, periods of steadier pressure occurred close to the initial transition from rain to snow, whereas steep pressure declines typically occurred almost simultaneously with the transition from snow to rain. Despite the systematic changes in pressure, surface winds were continually light in the storms. There was no distinct correlation between surface winds and the position of the rain–snow boundary.

There are several suggestions that can explain the disagreements between the observed precipitation type at the surface over southern Ontario and the predictions of Matsuo et al. (1981) from Japan. The presence of large snowflakes, as observed in the 13 May case, or substantially colder temperatures just above the surface would be consistent with the observations of snow in the mixed region (for both cases) and mixed precipitation in the rain region (13 May). Conversely, small snowflakes or relatively warm temperatures aloft would be consistent with the observation of rain in the mixed region (13 May). Because of a lack of suitable information, definitive conclusions can not be made on the causes of the discrepancies.

It is furthermore suggested that a mesoscale circulation was actually initiated by the melting process in the region of the rain–snow boundary. Circulations produced by melting have been described by several authors including Atlas et al. (1969) and Lin and Stewart (1986). Such a circulation is driven by a horizontal gradient in the diabatic cooling rate. In the case of a rain–snow boundary, this gradient of cooling would be expected to be greatest near the boundary as opposed to the rain region where melting is occurring everywhere or the snow region where it does not occur at all. A resulting mesoscale circulation is therefore predicted to be most pronounced near the rain–snow boundary. The exact locations of the updraft and downdraft regions of this circulation would depend on the horizontal distribution of the cooling, the horizontal temperature gradient throughout the lower troposphere in the boundary region, and on the ambient wind fields. The lack of appropriate mesoscale wind and temperature fields through the troposphere precludes a detailed comparison of predictions against observations. However, the general suggestion that updrafts must occur in the vicinity of the boundary are consistent with the present observations that the radar echo tops and the satellite derived cloud top heights were highest near the boundary.

5. Summary and concluding remarks

A rain–snow boundary is an important aspect of many Canadian storms. On the basis of an examination of storms having rain–snow boundaries, a number of observations and comments can be made.

The rain–snow boundaries demonstrated a number of characteristics. The width of the boundary varied substantially from about 11 km in the major storm examined to about 64 km in the weak storm studied. The boundary was either relatively constant in width, such as for the case of the major storm, or expanded, as in the weak storm. Although not observed here, it is also probable that the boundary could contract. The boundary's motion was similar to that of the winds at 1–3 km rather than surface or high-level winds. Surface temperature and pressure changes were linked to it. As well, the deepest radar echoes and the highest clouds as seen by satellite occurred close to its location. Perhaps as a consequence of the large snowflakes occurring near the boundary, at least some of the surface precipitation type observations were not consistent with similar observations made in Japan.

Some of the characteristics in the cases examined have been significantly affected by melting snow. Cooling the air by melting may be responsible for a significant portion of the observed surface temperature changes in the vicinity of the boundary. The deep radar

echoes and high clouds near the boundary may be a consequence of a mesoscale circulation driven by the horizontal gradient of melting. Some of the surface precipitation has undergone enhanced aggregation as it fell through a deep 0°C layer believed to occur in the boundary region, as well.

In summary, this study has examined some of the mesoscale and surface features of the rain–snow boundary. The boundary is a complex phenomenon in which the diabatic cooling by melting snow plays a significant role.

Acknowledgments. The authors would like to thank the reviewers and the editor, F. Sanders, for their constructive comments and suggestions.

REFERENCES

Atlas, D., R. Tatehira, R. C. Srivastava, W. Marker and R. E. Carbone, 1969: Precipitation-induced mesoscale wind perturbations in the melting layer. *Quart. J. Roy. Meteor. Soc.*, **95,** 544–560.

Battan, L. J., 1973: Radar Observations of the Atmosphere. University of Chicago Press, 324 pp.

Browning, K. A., and G. A. Monk, 1982: A simple model for the synoptic analysis of cold fronts. *Quart. J. Roy. Meteor. Soc.*, **108,** 435–452.

Carbone, R. E., 1982: A severe frontal rainband. Part I: Stormwide hydrodynamic structure. *J. Atmos. Sci.*, **39,** 258–279.

Findeisen, W., 1940: The formation of the 0°C isothermal layer and fractocumulus under nimbostratus. *Meteor. Z.*, **57,** 49–54.

Gunn, K. L. S., and J. S. Marshall, 1958: The distribution with size of aggregate snowflakes. *J. Meteor.*, **15,** 452–466.

Heymsfield, G. M., 1979: Doppler radar study of a warm frontal region. *J. Atmos. Sci.*, **36,** 2093–2107.

Koolwine, T., 1975: Freezing rain. M.Sc. thesis, University of Toronto, 92 pp.

Lamb, H. H., 1955: Two-way relationship between the snow or ice limit and 1000–5000 mb thickness in the overlying atmosphere. *Quart. J. Roy. Meteor. Soc.*, **81,** 172–189.

Leary, C. A., and R. A. Houze, Jr., 1979: Melting and evaporation of hydrometeors in precipitation from anvil clouds of deep tropical convection. *J. Atmos. Sci.*, **36,** 669–679.

Lin, C. A., and R. E. Stewart, 1986: Mesoscale circulations initiated by melting snow. *J. Geophys. Res.*, **91,** 13 299–13 302.

List, R., and J. G. Dussault, 1967: Quasi-steady state icing and melting conditions and heat and mass transfer of spherical and spheroidal hailstones. *J. Atmos. Sci.*, **24,** 522–529.

Lord, S. J., H. E. Willoughby and J. M. Piotrowicz, 1984: Role of a parameterized ice-phase microphysics in an axisymmetric, nonhydrostatic tropical cyclone model. *J. Atmos. Sci.*, **41,** 2836–2848.

Lumb, F. E., 1961: The problem of forecasting the downward penetration of snow. *Meteor. Mag.*, **90,** 310–319.

Marwitz, J. D., 1983: The kinematics of orographic airflow during Sierra storms. *J. Atmos. Sci.*, **40,** 1218–1227.

Matsuo, T., and Y. Sasyo, 1981a: Empirical formula for the melting rate of snowflakes. *J. Meteor. Soc. Japan,* **59,** 1–8.

——, and ——, 1981b: Melting of snowflakes below freezing level in the atmosphere. *J. Meteor. Soc. Japan,* **59,** 10–24.

——, and ——, 1981c: Non-melting phenomenon of snowflakes observed in subsaturated air below freezing level. *J. Meteor. Soc. Japan,* **59,** 26–32.

——, —— and Y. Sato, 1981: Relationship between types of precipitation on the ground and surface meteorological elements. *J. Meteor. Soc. Japan,* **59,** 462–476.

Ryde, J. W., 1946: The attenuation and radar echoes produced at centimeter wavelengths by various meteorological phenomena. *Meteorological Factors in Radio-Wave Propagation,* London, The Phys. Soc., 169–188.

Sanders, F., and J. R. Gyakum, 1980: Synoptic–dynamic climatology of the bomb. *Mon. Wea. Rev.*, **108,** 1589–1606.

Stewart, R. E., 1984: Deep 0°C isothermal layers within precipitation bands over southern Ontario. *J. Geophys. Res.*, **89,** 2567–2572.

——, 1985: Precipitation types in winter storms. *Pure Appl. Geophys.*, **123,** 597–609.

——, J. D. Marwitz, J. C. Pace and R. E. Carbone, 1984: Characteristics through the melting layer of stratiform clouds. *J. Atmos. Sci.*, **41,** 3227–3237.

Wexler, R., 1954: Precipitation growth in stratiform clouds. *Quart. J. Roy. Meteor. Soc.*, **72,** 363–371.

——, R. J. Reed and J. Honig, 1954: Atmospheric cooling by melting snow. *Bull. Amer. Meteor. Soc.*, **35,** 48–51.